Author Manuscript

Author Manuscript

Author Manuscript

Author Manuscript

HHS Public Access

Author manuscript

Nature. Author manuscript; available in PMC 2013 September 21.

Published in final edited form as:

Nature. 2013 March 21; 495(7441): 375–378. doi:10.1038/nature11940.

Multiple Phases of Chondrocyte Enlargement Underlie Differences in Skeletal Proportions

Kimberly L. Cooper[1,‡,*], **Seungeun Oh**[2,*], **Yongjin Sung**[3], **Ramachandra R. Dasari**[3], **Marc W. Kirschner**[2], and **Clifford J. Tabin**[1]

[1]Department of Genetics, Harvard Medical School, Boston, Massachusetts 02115, USA

[2]Department of Systems Biology, Harvard Medical School, Boston, Massachusetts 02115, USA

[3]George R. Harrison Spectroscopy Laboratory, Massachusetts Institute of Technology, Cambridge, Massachusetts 02139, USA

Abstract

Even a casual pass through the great halls of mammals in the world's natural history museums highlights the wide diversity of skeletal proportions that allow us to distinguish between species even when reduced to their calcified components. Similarly each individual is comprised of a variety of bones of differing lengths. The largest contribution to the lengthening of a skeletal element, and to the differential elongation of elements, comes from a dramatic increase in the volume of hypertrophic chondrocytes in the growth plate as they undergo terminal differentiation[1–7]. Despite this recognized importance, the mechanisms of chondrocyte volume enlargement have remained a mystery[8–11]. Here we use quantitative phase microscopy[12] to show that chondrocytes undergo three distinct phases of volume increase, including a phase of massive cell swelling in which the cellular dry mass is significantly diluted. In light of the tight fluid regulatory mechanisms known to control volume in many cell types[13], this stands as a remarkable mechanism for increasing cell size and regulating growth rate. It is, however, the duration of the final phase of volume enlargement by proportional dry mass increase at low density that varies most between rapidly and slowly elongating growth plates. Moreover, we find that this third phase is locally regulated through an Insulin-like Growth Factor-dependent mechanism. This study provides a framework for understanding how skeletal size is regulated and for exploring how cells sense, modify, and establish a volume set point.

Each of the long bones initially forms in the embryo as a similarly sized cartilage rudiment that only subsequently undergoes differential regulation of growth. The elongation of a skeletal element occurs at the growth plate[14,15], each consisting of three distinct zones:

Users may view, print, copy, download and text and data- mine the content in such documents, for the purposes of academic research, subject always to the full Conditions of use: http://www.nature.com/authors/editorial_policies/license.html#terms

‡Author for correspondence: kcooper@genetics.med.harvard.edu.

*These authors contributed equally to this work.

K.L.C. and S.O. conceived of the project and carried out the majority of the experiments. Y.S. and D.R. carried out critical spectroscopic experiments validating the primary approaches taken. C.J.T. and M.W.K. supervised the project. K.L.C., S.O., M.W.K. and C.J.T. wrote the manuscript.

The authors declare no competing financial interests.

Author Manuscript Author Manuscript Author Manuscript Author Manuscript

resting round chondrocytes near the end of an element give rise to clonal columns of flattened proliferating chondrocytes that then terminally differentiate into hypertrophic chondrocytes nearest the bony center of an element. While multiple cellular parameters contribute to lengthening of skeletal elements - including proliferation, matrix deposition, and hypertrophic cell enlargement - the greatest contribution to growth rate in mammals is due to the massive volume enlargement of hypertrophic chondrocytes expanding the skeletal tissue in the direction of longitudinal growth within laterally restricting matrix channels[1–3]. In addition to being the largest contributor to the elongation rate of a given skeletal element, this parameter is largely responsible for the difference in growth rates between different skeletal elements within an individual, between homologous elements in different species, and within a single element as an animal ages[4–7]. Surprisingly, however, given its critical importance in determining the growth rate of each bone and the overall stature of the individual, the mechanism is poorly understood. It even remains unclear whether hypertrophic chondrocyte volume increases by true hypertrophy, maintaining constant density during growth through an increase in macromolecules and organelles, or by cell swelling via disproportionate fluid uptake which is ordinarily a hallmark of disease[13].

To determine whether hypertrophic chondrocytes enlarge by cellular hypertrophy and/or swelling, we applied methods of diffraction phase microscopy to measure the dry mass of individual unstained live cells dissociated from growth plate cartilage. (Fig. 1a; Supplementary Methods)[16]. Together with volume information about the sample, calculated here based on a well-supported spherical approximation for dissociated chondrocytes (Supplementary Methods), this allows the calculation of dry mass density. Diffraction phase microscopy measurements of a variety of cell types consistently reflect a “normal” dry mass density for healthy living cells at approximately 0.182 pg/fl in agreement with the concentration of cytoplasm previously determined by index matching in human oral epithelial cells[17]. This includes maturing megakaryocytes that reach volumes comparable to the largest hypertrophic chondrocytes and ten-times the average somatic cell volume (Supplementary Fig. S1).

In contrast, analysis of chondrocytes from the rapidly elongating mouse proximal tibia reveals that there are three distinct phases of hypertrophic cell enlargement. 1) An initial increase of about 3-fold from approximately 600 fl to 2000 fl is characterized by true hypertrophy - a proportionate increase in dry mass production and fluid uptake thus maintaining the normal dry mass density at 0.183 pg/fl (Fig. 1b, c). 2) A second phase where a 4-fold enlargement from about 2000 fl to 8000 fl is characterized by cell swelling. Volume increases at a rate disproportionate to the continuing rate of dry mass production resulting in a dramatic dilution of dry mass density to approximately 0.07 pg/fl (Fig. 1c). 3) At volumes larger than 8000 fl, the dry mass density once again stabilizes, and cells continue to enlarge another 2-fold to about 14,000 fl by proportionately increasing dry mass and fluid volume at this lower density (Fig. 1d). Swelling in Phase 2 allows cells to reach volumes two to three times greater in Phase 3 than if they relied entirely on the proportionate increase in dry mass at high density (Fig. 1b, linear regression).

To verify that this decrease in density is characteristic of hypertrophic differentiation, we imaged a subset of the small high-density cells and large low-density cells using regularized

Author Manuscript Author Manuscript Author Manuscript Author Manuscript

tomographic phase microscopy to generate a refractive index map of dry mass density in three-dimensions (Supplementary Methods). This independent approach confirms that the largest cells reduce their dry mass density by approximately 60%, and moreover indicates that dry mass is low throughout the cytoplasm with a slightly higher density ring around the nucleus (Fig. 1e, f; Supplementary Fig. S14).

Understanding the cellular process by which hypertrophic cells enlarge provides a framework for considering how that process is modulated to achieve differential growth of individual elements within a species and of homologous elements between species. In contrast to the large hypertrophic chondrocytes of the rapidly elongating proximal tibia, the slowly elongating proximal radius has much smaller hypertrophic chondrocytes[1]. We find that these cells go through Phase 1 and enter Phase 2 similar to the cells of the proximal tibia, reaching a volume of approximately 5,000 fl. However, they truncate the remainder of Phase 2 after dilution of dry mass density to approximately 0.10 pg/fl and completely eliminate Phase 3 (Fig. 2a).

We next compared growth plates of the mouse to those of the jerboa, a small bipedal rodent with greatly elongated hindlimbs. In particular, the metatarsals of the feet rapidly elongate during early postnatal development to approximately 2.5 times the relative proportion of mouse metatarsals[18]. The mouse distal metatarsal growth plate is intermediate in its growth rate and hypertrophic chondrocyte size relative to the proximal tibia and radius (Fig. 2b; Supplementary Fig. S2). While other aspects of the jerboa distal metatarsal growth plate are also altered, including the total cell number in each zone (Supplementary Fig. S3), the height of individual hypertrophic chondrocytes is increased by 58% compared to those in the homologous growth plate of the mouse suggesting a significant contribution of hypertrophic chondrocyte volume to the increased rate of growth of this element (Fig. 2b, e, f). In contrast, the jerboa tibia hypertrophic chondrocytes are only slightly larger than their counterparts in the mouse (Fig. 2b, c, d). Unlike the metatarsals, the metacarpals of the jerboa forelimb, as well as other bones of the forelimb, are similar in size and proportions to those of the mouse with hypertrophic chondrocytes of comparable size (Fig. 2b).

The hypertrophic chondrocytes of the jerboa proximal tibia show very similar growth properties to those of the mouse when examined by diffraction phase microscopy, including all three phases of volume enlargement (Supplementary Fig. S4). However, there is a striking difference between the metatarsal chondrocytes of the two species. Mouse metatarsal hypertrophic chondrocytes are indeed intermediate in size between the proximal radius and proximal tibia, reaching a maximum volume of about 8000 fl by completing Phases 1 and 2 and truncating Phase 3 (Fig. 2g). Hypertrophic chondrocytes of the jerboa metatarsals increase almost 40-fold from their initial volume to approximately 23,000 fl, greater than the volume of tibia chondrocytes in either species (Fig. 2h). This is accomplished by following the same tri-phasic growth trajectory common to chondrocytes of other growth plates and then extending Phase 3 to reach a maximal volume by continued proportionate increase in dry mass and fluid volume at low dry mass density.

Little is known about the molecular mechanisms that control chondrocyte enlargement, or the regulation of final cell size, since few of the mutants affecting skeletal development have

Author Manuscript Author Manuscript Author Manuscript Author Manuscript

been examined for size of individual hypertrophic chondrocytes. An intriguing exception is the null mutation of the gene encoding Insulin-like Growth Factor 1 (*Igf1*)[19]. *Igf1* functions in a variety of target tissues to promote protein synthesis and cell growth[19,20] and is strongly expressed in both proliferating and pre-hypertrophic chondrocytes. *Igf1*-deficient mice are 35% smaller than controls but have the same number of hypertrophic chondrocytes, though each cell is 30% shorter in the direction of elongation, a finding we confirmed in mice where the floxed *Igf1*^{tm1Dlr} allele[21] was conditionally deleted from the hindlimb using *HoxB6-Cre*[22] (Fig. 3a–c). It is additionally intriguing to note that there is no distinction between the heights of chondrocytes in the proximal tibia and distal metatarsal of this mutant (Fig. 3c) indicating that *Igf1* may play an important role in the establishment of growth plate dependent cell size. While this effect could be modulated by any member of the *Igf1* signaling pathway, evidence suggests a possible role for the receptor, *Igf1R*, that maintains higher levels of expression over time in growth plates that continue to elongate at faster rates in maturing mice[23].

We employed diffraction phase microscopy to determine which phase(s) of volume enlargement are affected by *Igf1*. *Igf1*-deficient hypertrophic chondrocytes undergo normal Phase 1 and Phase 2 of enlargement, reaching approximately 7000 fl largely by cell swelling, but do not progress to Phase 3 and thus fail to further double their volume by the continued production of dry mass at low density (Fig. 3d–f). Taken together, our results indicate that there are three distinct phases of chondrocyte hypertrophy, and it is regulation of the *Igf1*-dependent third phase that is responsible for much of the variation in skeletal elongation rate.

Finally, previous studies of the neonatal bat and mouse forelimb suggested that the entire hypertrophic zone of each growth plate turns over once in about 24 hours regardless of the maximum volume attained by individual chondrocytes, the number of hypertrophic chondrocytes, or rate of growth plate elongation[7]. This suggests that growth plates elongating at different rates adjust the rate of cell volume increase to fall within a 24-hour lifespan constraint. To assess the pace of cellular maturation and enlargement, we marked proliferating chondrocytes with BrdU and followed the progression of the first labeled cells to emerge into the postmitotic hypertrophic columns onward to the chondro-osseous junction (Supplementary Fig. S5). We find that the rate of cell height increase in both growth plates is extremely rapid, more than tripling the height of proximal tibia chondrocytes within approximately 12 hours (Fig. 4a). Once cells reach their average final height, with a steeper slope in the larger cells of the tibia, they remain at this terminal size in the hypertrophic growth columns for an additional 12 hours before turnover at the chondro-osseous junction.

Through coordination of this multiphase process, cell swelling allows chondrocytes to enlarge extraordinarily rapidly while presumably lowering the energetic cost of growth, and volumes are subsequently amplified in the most rapidly elongating skeletal elements by the continued *Igf1*-dependent production of mass. This unique mechanism of volume enlargement suggests that chondrocyte hypertrophy will serve as a valuable model for cell volume homeostasis, in addition to our findings that provide insight into skeletal morphogenesis and evolution.

Author Manuscript Author Manuscript Author Manuscript Author Manuscript

Full Methods

Animals

CD-1 was chosen as the wild type mouse strain for this study. *Igf1*^{tm1Dlr} conditional mice[21] and *HoxB6-Cre* transgenic mice[22] were previously described. Jerboas were housed and reared as previously described[24]. All animal protocols were approved by the Harvard Medical Area Standing Committee on Animals.

Sectioning and histology

Dissected skeletal elements were fixed overnight at 4°C in 4% paraformaldehyde and then carried through a graded series of ethanol dehydration washes before transition through xylenes and into paraffin wax. Sections were cut at 10–12 μm thickness and stained with hematoxylin and eosine. Average maximum cell heights were measured in the axis of linear growth through the lacunae surrounding the largest cells with a clear nuclear profile from digital images of the hypertrophic zone and averaged across at least 4 sections from at least 3 individuals. Bromodeoxyuridine (100 mg/kg) or oxytetracycline hydrochloride (20 mg/kg) was injected into the peritoneum of postnatal day 5 mice before harvest. BrdU was detected using a rat anti BrdU (AbD Serotech) followed by goat anti-rat Alexa594 (Invitrogen) in paraffin sections. Oxytetracycline was detected by fluorescence in bisected skeletal elements.

Chondrocyte and megakaryocyte isolation

Postnatal day 5 animals were chosen for this study because the tibia and metatarsal growth plates are rapidly elongating in both species, but the metatarsal epiphysis (secondary ossification center) has not yet formed. While the epiphysis of the metatarsal forms by P7 in the mouse, it appears later in the jerboa (Fig. S3). Since the hypertrophic chondrocytes reside in a small domain nearest the chondro-osseous junction, we enriched for these cells by using a razor blade to remove a majority of the cartilage containing resting and proliferative chondrocytes leaving the cells closest to the chondro-osseous junction and a small amount of the adjacent trabecular bone. Growth plates were bisected longitudinally and incubated for 45 minutes at 37°C in 2 mg/ml Collagenase D (Roche) in DMEM/F12 (Invitrogen, 290–330 mOsm) plus 10% fetal calf serum. After the initial incubation, the bone collar, trabecular bone, and loosened connective tissues were manually removed with forceps, and the remaining cartilage fragments were transferred to a fresh dish of collagenase digestion media. Cells were incubated for an additional 2–3 hours with occasional swirling until cells mostly dissociated from the surrounding matrix. Dissociated chondrocytes were transferred to 35 mm dishes with a 14 mm diameter, 1.5-thickness glass bottom (MatTek) and imaged immediately. The largest hypertrophic chondrocytes are a small population of the most mature cells, therefore we further enriched for this population in our data analysis by scanning for fields of view containing the largest cells in the dish and quantified all of the intact spherical neighbors.

There has been a longstanding discussion in the literature regarding the extracellular osmolarity of chondrocytes, primarily in the articular cartilage[9,10,25,26]. Much of this data is based on the theoretical ionic environment in association with charged glycosaminoglycans

Author Manuscript Author Manuscript Author Manuscript Author Manuscript

according to the Donnan-Gibbs equilibrium, though to our knowledge the extracellular osmolarity of growth plate cartilage has not been directly measured. While serum osmolarity is approximately 280 mOsm, the osmolarity in association with cartilage may be upwards of 400 mOsm. To address the possibility that the swelling we observe in chondrocytes at larger volumes may be the response to media of low osmolarity, we repeated the diffraction phase microscopy measurements in mouse proximal tibia growth plates dissociated in 424 mOsm DMEM/F12 raised with sucrose. Media osmolarity was measured using the Vapro Model 5600 (Wescor, Inc). We find the same three phases, including the phase of cell swelling, indicating this is an inherent property of growth plate chondrocytes and not the passive response to an abnormal osmotic environment (Fig. S6). We presume that the 4 hours from dissection to imaging is enough time for volume regulatory mechanisms to compensate for any response to osmotic stress that may have occurred. Indeed, 4-D confocal imaging of in situ porcine articular chondrocytes after osmotic stress shows a mean recovery rate of 4.1% ±1.8%/min with 96% volume recovery after about 12 minutes[27].

Fetal megakaryocytes were isolated from embryonic day 14.5 mouse livers according to previously published protocols[28,29] or generously donated by Dr. Annouck Luyten and Dr. Ramesh Shivdasani. Cells were imaged by DPM one day after harvest or at maturity after five days in culture.

Supplementary Material

Refer to Web version on PubMed Central for supplementary material.

Acknowledgments

We would like to thank T.J. Mitchison, C.E. Farnum, and members of the Developmental Bone Morphogenesis program project grant (NIH) for helpful discussions. We also thank the Nikon Imaging Center at Harvard Medical School for technical support, A. Luyten and R. Shivdasani for providing mouse megakaryocytes, and P. Ramirez for jerboa care. This work was supported by National Institutes of Health (NIH) grants P01DK056246 to C.J.T, R01GM026875 to M.W.K., and by NIH grant P41RR02594, National Science Foundation (NSF) grant DBI0754339 and support from the Hamamatsu Corporation to R.R.D.

References

1. Wilsman NJ, Farnum CE, Leiferman EM, Fry M, Barreto C. Differential growth by growth plates as a function of multiple parameters of chondrocytic kinetics. J Orthop Res. 1996; 14:927–36. [PubMed: 8982136]
2. Hunziker EB, Schenk RK, Cruz-Orive LM. Quantitation of chondrocyte performance in growth-plate cartilage during longitudinal bone growth. J Bone Joint Surg Am. 1987; 69:162–173. [PubMed: 3543020]
3. Hunziker EB, Schenk RK. Physiological mechanisms adopted by chondrocytes in regulating longitudinal bone growth in rats. J Physiol (Lond). 1989; 414:55–71. [PubMed: 2607442]
4. Breur GJ, VanEnkevort BA, Farnum CE, Wilsman NJ. Linear relationship between the volume of hypertrophic chondrocytes and the rate of longitudinal bone growth in growth plates. J Orthop Res. 1991; 9:348–359. [PubMed: 2010838]
5. Kuhn JL, Delacey JH, Leenellett EE. Relationship between bone growth rate and hypertrophic chondrocyte volume in new zealand white rabbits of varying ages. Journal of Orthopaedic Research. 1996; 14:706–711. [PubMed: 8893762]

Author Manuscript Author Manuscript Author Manuscript Author Manuscript

6. Wilsman NJ, Bernardini ES, Leiferman E, Noonan K, Farnum CE. Age and pattern of the onset of differential growth among growth plates in rats. J Orthop Res. 2008; 26:1457–1465. [PubMed: 18404738]
7. Farnum CE, Tinsley M, Hermanson JW. Forelimb versus Hindlimb Skeletal Development in the Big Brown Bat, *Eptesicus fuscus*: Functional Divergence Is Reflected in Chondrocytic Performance in Autopodial Growth Plates. Cells Tissues Organs. 2008; 187:35–47. [PubMed: 18160801]
8. Buckwalter JA, Mower D, Ungar R, Schaeffer J, Ginsberg B. Morphometric analysis of chondrocyte hypertrophy. J Bone Joint Surg Am. 1986; 68:243–255. [PubMed: 3944163]
9. Farnum CE, Lee R, O'Hara K, Urban JPG. Volume increase in growth plate chondrocytes during hypertrophy: the contribution of organic osmolytes. Bone. 2002; 30:574–581. [PubMed: 11934648]
10. Bush PG, Parisinos CA, Hall AC. The osmotic sensitivity of rat growth plate chondrocytes in situ; clarifying the mechanisms of hypertrophy. J Cell Physiol. 2008; 214:621–629. [PubMed: 17786946]
11. Bush PG, Pritchard M, Loqman MY, Damron TA, Hall AC. A key role for membrane transporter NKCC1 in mediating chondrocyte volume increase in the mammalian growth plate. J Bone Miner Res. 2010; 25:1594–1603. [PubMed: 20200963]
12. Barer R. Interference microscopy and mass determination. Nature. 1952; 169:366–367. [PubMed: 14919571]
13. Hoffmann EK, Lambert IH, Pedersen SF. Physiology of cell volume regulation in vertebrates. Physiol Rev. 2009; 89:193–277. [PubMed: 19126758]
14. Hunziker EB. Mechanism of longitudinal bone growth and its regulation by growth plate chondrocytes. Microsc Res Tech. 1994; 28:505–519. [PubMed: 7949396]
15. Kronenberg H. Developmental regulation of the growth plate. Nature. 2003; 423:332–336. [PubMed: 12748651]
16. Popescu G, Ikeda T, Dasari RR, Feld MS. Diffraction phase microscopy for quantifying cell structure and dynamics. Opt Lett. 2006; 31:775–777. [PubMed: 16544620]
17. Barer R. Determination of Dry Mass, Thickness, Solid and Water Concentration in Living Cells. Nature. 1953; 172:1097–1098. [PubMed: 13111263]
18. Cooper KL. The lesser Egyptian jerboa, Jaculus jaculus: a unique rodent model for evolution and development. Cold Spring Harb Protoc. 2011; 2011:1451–1456. [PubMed: 22135653]
19. Wang J, Zhou J, Bondy CA. Igf1 promotes longitudinal bone growth by insulin-like actions augmenting chondrocyte hypertrophy. FASEB J. 1999; 13:1985–1990. [PubMed: 10544181]
20. Oldham S, Hafen E. Insulin/IGF and target of rapamycin signaling: a TOR de force in growth control. Trends in Cell Biology. 2003; 13:79–85. [PubMed: 12559758]
21. Yakar S. Normal growth and development in the absence of hepatic insulin-like growth factor I. Proceedings of the National Academy of Sciences. 1999; 96:7324–7329.
22. Lowe LA, Yamada S, Kuehn MR. HoxB6-Cre transgenic mice express Cre recombinase in extra embryonic mesoderm, in lateral plate and limb mesoderm and at the midbrain/hindbrain junction. genesis. 2000; 26:118–120. [PubMed: 10686603]
23. Serrat MA, Lovejoy CO, King D. Age- and site-specific decline in insulin-like growth factor-I receptor expression is correlated with differential growth plate activity in the mouse hindlimb. Anat Rec (Hoboken). 2007; 290:375–381. [PubMed: 17514762]
24. Jordan B, Vercammen P, Cooper KL. Husbandry and breeding of the lesser Egyptian Jerboa, Jaculus jaculus. Cold Spring Harb Protoc. 2011; 2011:1457–1461. [PubMed: 22135654]
25. Maroudas A, Evans H. A Study of Ionic Equilibria in Cartilage. Connective Tissue Research. 1972; 1:69–77.
26. Urban JPG, Hall AC, Gehl KA. Regulation of matrix synthesis rates by the ionic and osmotic environment of articular chondrocytes. Journal of Cellular Physiology. 1993; 154:262–270. [PubMed: 8425907]
27. Errington RJ, Fricker MD, Wood JL, Hall AC, White NS. Four-dimensional imaging of living chondrocytes in cartilage using confocal microscopy: a pragmatic approach. Am J Physiol. 1997; 272:C1040–1051. [PubMed: 9124506]

Author Manuscript Author Manuscript Author Manuscript Author Manuscript

28. Lecine P, Blank V, Shivdasani R. Characterization of the hematopoietic transcription factor NF-E2 in primary murine megakaryocytes. J Biol Chem. 1998; 273:7572–7578. [PubMed: 9516460]
29. Shivdasani, RA.; Schulze, H. Culture, Expansion, and Differentiation of Murine Megakaryocytes.

Author Manuscript Author Manuscript Author Manuscript Author Manuscript

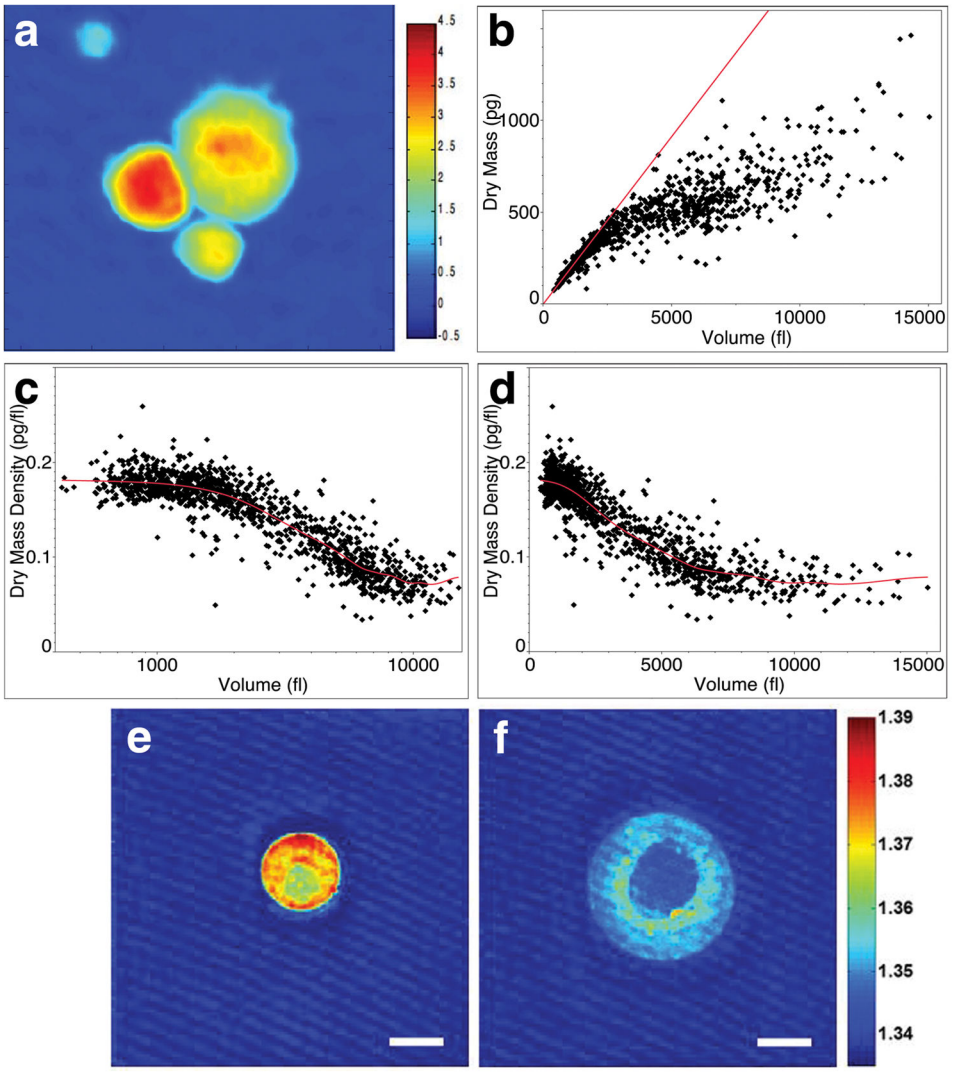

Figure 1. Hypertrophic chondrocytes increase in volume through three distinct phases including a phase of massive cell swelling

a, Phase image of dissociated mouse proximal tibia hypertrophic chondrocytes at postnatal day 5 (P5). Color bar represents phase shift in radians. b, Volume versus dry mass plotted for individual chondrocytes. Linear regression for cells up to 1,000 fl highlights divergence of larger cells from an initial slope of 0.183 pg/fl. Log scale (c) and linear scale (d) plots of volume versus dry mass density. Lambda for the smoothened spline in (c) and (d) is 5e+9. R^2 value is 0.84. n=1249 cells summed across five independent experiments. e, f, Horizontal cross sections from regularized tomographic phase microscopy density reconstructions of a small (e) and a large (f) mouse tibia chondrocyte. Color bar represents refractive index and thus dry mass density. Scale bar is 10 μm.

Author Manuscript Author Manuscript Author Manuscript Author Manuscript

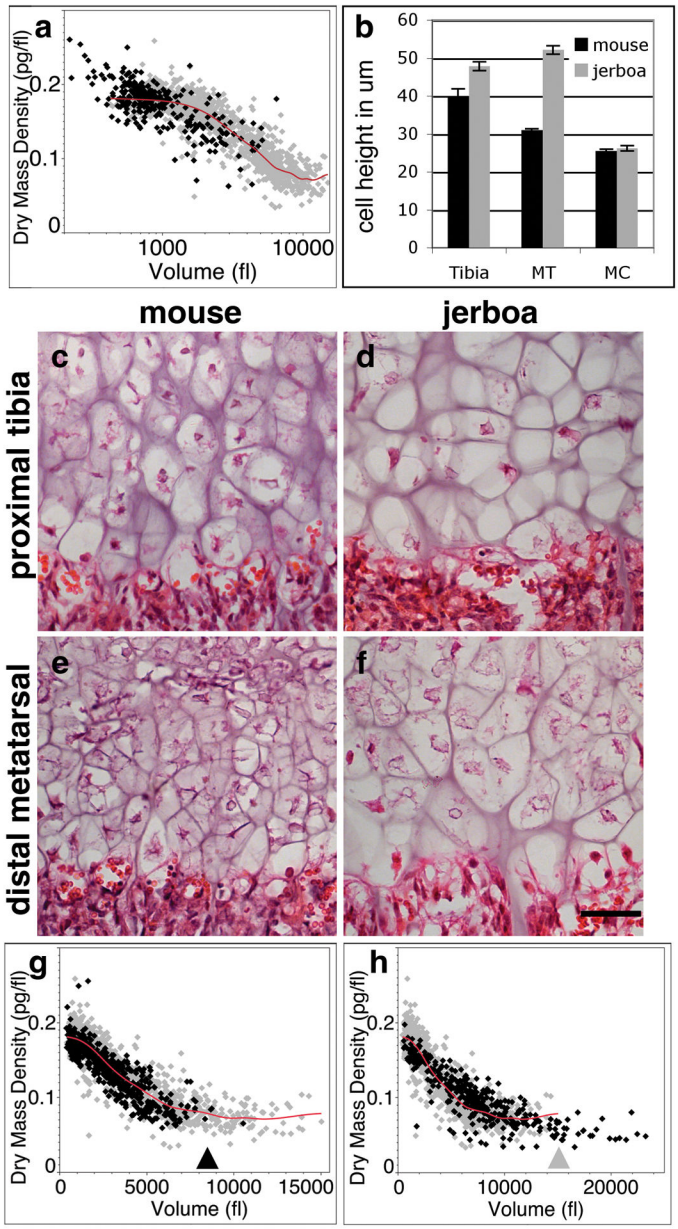

Figure 2. Differences in cell size associated with different skeletal growth rates are attributed to modulating a common growth trajectory

a, Dissociated P5 mouse proximal radius chondrocytes (black; n=292 cells) compared to proximal tibia chondrocytes (gray in all panels; data from Fig. 1). x-axis is in log scale. b, Quantification of average maximum cell height ± s.e.m for n=3 animals of each species at P7 (>50 cells per growth plate). Two-tailed student's t-test shows significant differences in the tibia and metatarsal growth plates between the two species ($p<10^{-5}$) but not in the metacarpals (p=0.978). c–f, Histological comparison of mouse and jerboa proximal tibia and distal metatarsal hypertrophic zones at P7. Scale bar equals 50 μm. g, Dissociated P5 mouse metatarsal chondrocytes (black; n=634 cells) compared to mouse tibia chondrocytes. Black arrowhead approximates the end of the metatarsal distribution h, Jerboa metatarsal

chondrocytes (black; n=366 cells) compared to mouse tibia chondrocytes. Grey arrowhead approximates the end of the mouse tibia distribution.

Author Manuscript Author Manuscript Author Manuscript Author Manuscript

Author Manuscript Author Manuscript Author Manuscript Author Manuscript

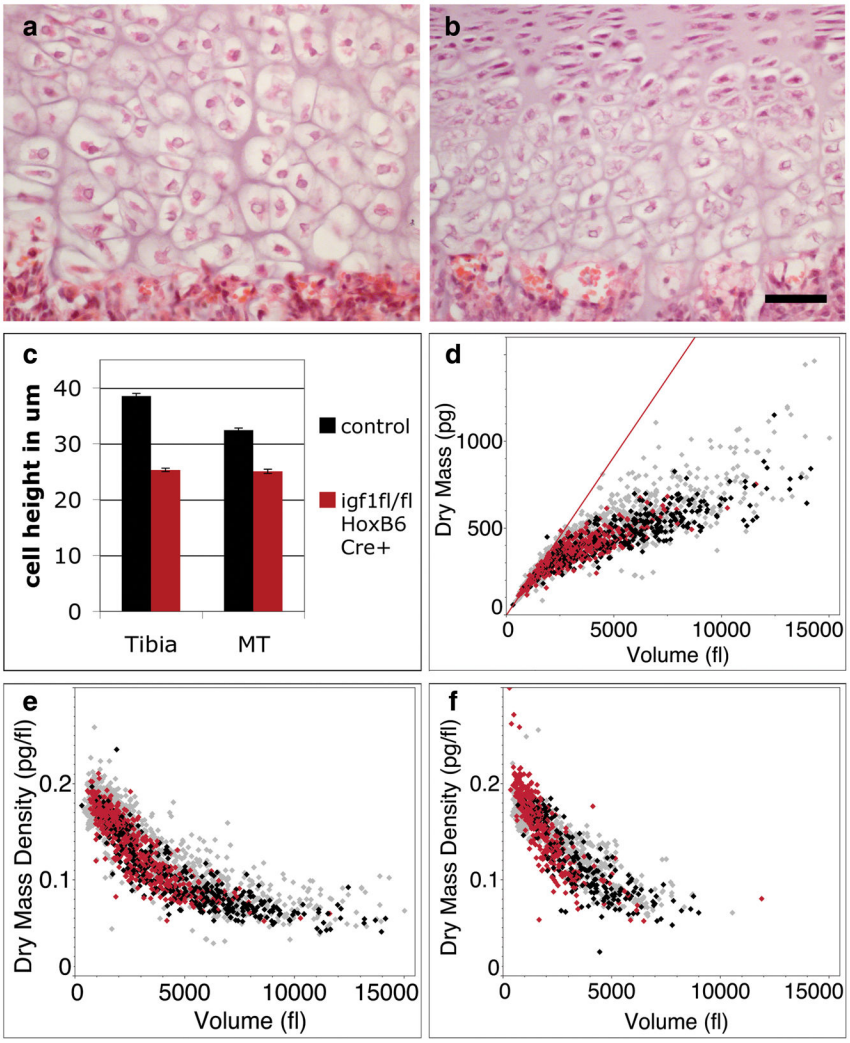

Figure 3. *Igf1* is required for Phase 3 of volume enlargement by dry mass production at low dry mass density

a, b, Histology of P7 mouse proximal tibia hypertrophic zone of control (**a,** *igf1*$^{fl/+}$; HoxB6-Cre^{+}) and *igf1* conditional mutant animals (**b,** *igf1*$^{fl/fl}$; HoxB6-Cre^{+}). Scalebar equals 50 μm. **c,** Bar plot demonstrating an average maximum cell height reduction of 34% in *igf1* conditional mutant tibia and 23% in metatarsal chondrocytes compared to control litter mates. ± s.e.m. for n=3 animals of each genotype (total >80 cells per growth plate). **d**, Dry mass versus volume plot of dissociated P5 *igf1* mutant proximal tibia hypertrophic chondrocytes. Red datapoints are *igf1* mutant chondrocytes (n=569 cells), black are littermate control chondrocytes (n=373 cells), and grey represent the total wild-type data set for tibia (**d, e**) and metatarsal (**f**) (wild-type data from Fig. 1 and Fig. 2). **e, f,** Dry mass density versus volume plots for *igf1* mutant tibia chondrocytes (n=569 cells) (**e**) and *igf1* mutant metatarsal chondrocytes (n=412 cells) (**f**).

Author Manuscript Author Manuscript Author Manuscript Author Manuscript

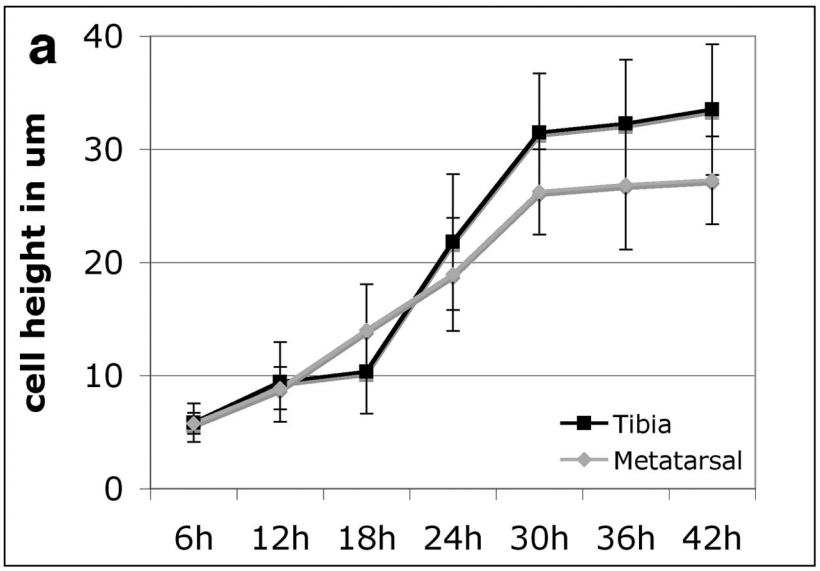

Figure 4. Mouse proximal tibia and distal metatarsal hypertrophic chondrocytes rapidly increase in average cell height

a, Time course of the average and standard deviation of BrdU labeled cell height indicating the rate of chondrocyte size increase after the last mitotic cycle. n>25 cells from three individuals for each time point and growth plate.